Computers in Biology and Medicine 43 (2013) 1661–1672

Contents lists available at ScienceDirect

Computers in Biology and Medicine

journal homepage: www.elsevier.com/locate/cbm

Multi-Gaussian fitting for pulse waveform using Weighted Least Squares and multi-criteria decision making method

Lu Wang [a], Lisheng Xu [b,c,*], Shuting Feng [b], Max Q.-H. Meng [d], Kuanquan Wang [e]

[a] College of Information Science and Engineering, Northeastern University, Shenyang City, Liaoning Province, 110819, China
[b] Sino-Dutch Biomedical and Information Engineering School, Northeastern University, Shenyang City, Liaoning Province, 110819, China
[c] Key Laboratory of Medical Image Computing (Northeastern University), Ministry of Education, China
[d] Department of Electronic Engineering, Chinese University of Hong Kong, Hong Kong, China
[e] School of Computer Science and Technology, Harbin Institute of Technology, Harbin 150001, China

ARTICLE INFO

Article history:
Received 15 November 2012
Accepted 11 August 2013

Keywords:
Pulse waveform
Photoplethysmography
Pulse decomposition analysis
Multi-Gaussian model
Multi-criteria decision making

ABSTRACT

Analysis of pulse waveform is a low cost, non-invasive method for obtaining vital information related to the conditions of the cardiovascular system. In recent years, different Pulse Decomposition Analysis (PDA) methods have been applied to disclose the pathological mechanisms of the pulse waveform. All these methods decompose single-period pulse waveform into a constant number (such as 3, 4 or 5) of individual waves. Furthermore, those methods do not pay much attention to the estimation error of the key points in the pulse waveform. The estimation of human vascular conditions depends on the key points' positions of pulse wave. In this paper, we propose a Multi-Gaussian (MG) model to fit real pulse waveforms using an adaptive number (4 or 5 in our study) of Gaussian waves. The unknown parameters in the MG model are estimated by the Weighted Least Squares (WLS) method and the optimized weight values corresponding to different sampling points are selected by using the Multi-Criteria Decision Making (MCDM) method. Performance of the MG model and the WLS method has been evaluated by fitting 150 real pulse waveforms of five different types. The resulting Normalized Root Mean Square Error (NRMSE) was less than 2.0% and the estimation accuracy for the key points was satisfactory, demonstrating that our proposed method is effective in compressing, synthesizing and analyzing pulse waveforms.

1. Introduction

The arterial pulse waves in all their forms, pressure, volume or flow, contain the information about the cardiovascular system such as heart rate, pulsatile pressure and arterial distensibility; therefore, they are often used by clinicians in the assessment of health and the early prediction of cardiovascular diseases. The arterial pulse wave is generated by the heart and propagated through the arterial tree. The increase in blood volume in the artery causes a transient increase in pressure which depends on the property of the arterial wall as well as the resistance of the peripheral vessels and tissues. Sphygmograph, an instrument for graphically recording the form, strength, and variations of the arterial pulse, was developed in 1854 by the German physiologist Karl von Vierordt (1818–1884). Currently, it has been employed as an external, noninvasive device to record the pressure pulse wave and to estimate the blood pressure. Photoplethysmograph (PPG), an optical, non-invasive, and easy-to-obtain technique, has been used for capturing Digital Volume Pulse (DVP) signals from peripheral pulse sites (e.g. fingers, earlobes, toes etc) [1–3]. Despite the fact that the morphologies of pulse waveforms acquired by different kinds of sensors at different sites vary greatly, they all contain similar information of peripheral pulse waves [3] and can provide important clinical information related to the conditions of the cardiovascular system [4–7].

A single period of pulse wave is composed of an ascending limb and a descending limb, as illustrated in Fig. 1. The percussion wave consists of a portion of the ascending limb and a portion of the descending limb of a pulse wave; the tidal wave, dicrotic notch and dicrotic wave constitute the remaining portion of the descending limb of a pulse wave. Prior to the dicrotic notch, the wave reflects the condition of heart systole, whereas the wave after the notch reflects the condition of the periphery. Peripheral resistance can influence the dicrotic wave. Arterial compliance also has a notable influence on pulse waves. The key points such as the crests and troughs of pulse waveform contain clinic information on human cardiovascular systems. Similar to the constitution of the

* Corresponding author at: Sino-Dutch Biomedical and Information Engineering School, Northeastern University, Shenyang City, Liaoning Province, 110819, China. Tel.: +86 24 83683200; fax: +86 24 83681955.
E-mail address: xuls@bmie.neu.edu.cn (L. Xu).

0010-4825/$ - see front matter © 2013 Elsevier Ltd. All rights reserved.
http://dx.doi.org/10.1016/j.compbiomed.2013.08.004

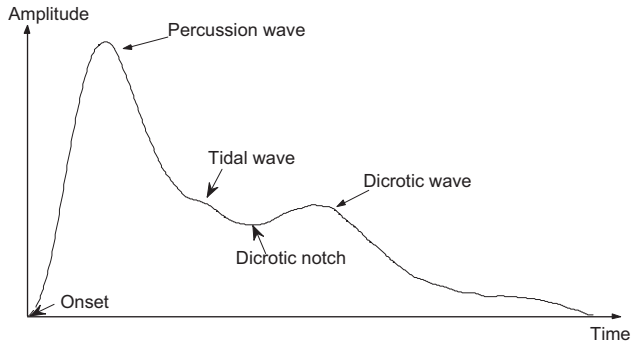

Fig. 1. Schematic figure of pulse wave.

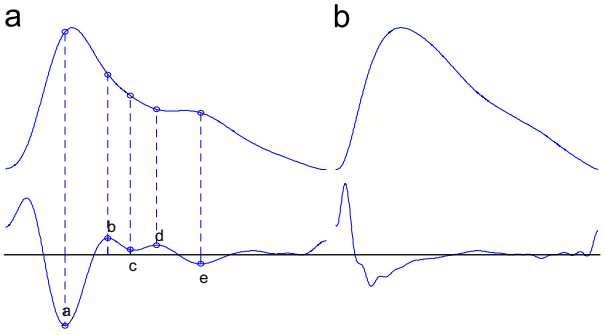

Fig. 2. Digital volume pulse (DVP) (upper panel) and its second derivative (lower panel). (a) The illustration of *a*, *b*, *c*, *d* and *e* waves in SDDVP and (b) the five waves do not always exist in SDDVP.

peripheral pressure pulse wave, a DVP waveform comprises a systolic component arising from pressure waves propagated from the aortic root to the finger and a diastolic component arising from pressure waves reflected backward from peripheral arteries mainly in the lower body, which then propagate to the finger. The reflected waves produce an inflection point or second crest in the DVP [8,21–23].

Commonly used parameters of DVP are pulse duration, Augmentation Index (AI), Reflection Index (RI), Pulse Transit Time (PTT), Pulse Wave Velocity (PWV) and so on [8]. There are other ways to assess some of these parameters, such as CT, MRI, and ultrasound techniques [4,9]. However, these methods are more expensive and less convenient than the measurement and analysis of peripheral pulse waveforms. Therefore, many methods for pulse parameter estimation based on peripheral pulse waveforms have been proposed [10–18].

The Double Differentiation analysis [10–12,19] was applied to estimate pulse parameters from the five sequential waves called *a*, *b*, *c*, *d* and *e* waves (Fig. 2(a)), which are demonstrated in the Second Derivative of Digital Volume Pulse (SDDVP), defined as d^2DVP/dt^2, sometimes being named as the acceleration photoplethysmogram. The advantage of this method is its simplicity and the possibility to be used in real-time. But its performance will degrade when the DVP signal is weak and noisy, especially when the diastolic part of the DVP waveform monotonically decreases [12]. As shown in Fig. 2(b), the *a*, *b*, *c*, *d* and *e* waves, which are notable in Fig. 2(a), cannot be easily detected from the DVP shown in Fig. 2(b).

In order to extract some features from the pulse wave more effectively, the Pulse Decomposition Analysis (PDA) method, which decomposes a pulse waveform into several individual component waves, has been developed in recent years [13]. This method extracts the parameters by fitting DVP waveform with four or more individual waves [13–15,24–29]. At present, several different PDA methods have been proposed, some of which decompose DVP waveform into two components for compressing and analyzing [4,14–20], such as the attempt by Westerhof et al. to separate a pressure pulse wave into two parts by a triangular wave of duration equal to the ejection time [16]. Jan G. Kips et al. proved that an approximation of reflected wave by using a triangular flow wave had limited accuracy [17], then they proposed a physiological flow wave approximation method, which yields a significantly better agreement between approximated and actual Reflection Magnitude (RM), but considerable deviations still persist [17]. A Two-Pulse Synthesis (TPS) model presented by Goswami et al. [4] successfully reconstructed DVP waveforms using Raleigh functions with small Mean Square Error (MSE), which is less than 0.005 when the amplitude of DVP waveform is normalized; but when three or more crests exist in the DVP waveform, the TPS model fails.

A Gaussian wave has a similar morphology to the pulsatile components in a pulse wave and the Gaussian model is very efficient in that a relatively complex waveform can be represented by using a very small set of parameters, allowing the pulse wave to be represented by a combination of Gaussian waves [13–15,24–27]. Qian Weili et al. decomposed a pulse wave into three Gaussian waves for synthesis [13]. Rubins et al. explored the use of two or four Gaussian waves to synthesize and to approximate a portion of or the whole of a DVP waveform [14]. Martin C. Baruch et al. proposed a new PDA model of arterial pulse wave by decomposing it into five individual pulses [15]. Two parameters, transit time of the reflected wave (RTT) and Augmentation Index (AIx), are calculated by analyzing time intervals between the crests of these individual pulses and the amplitude relation of these crests [15]. However, these researches pay no attention to the fitting accuracy in those key points of pulse wave. Actually, the fitting error of these crests can greatly influence the calculation of the parameters such as RTT, AIx and so on.

All the methods mentioned above separate a DVP wave into two or more waves, but they all have limitations in terms of accuracy [16,17] or flexibility [4,15,24–27]. In order to develop a simple and effective algorithm for extracting component waves of DVP, an adaptive Multi-Gaussian (MG) model is proposed to fit DVP waveform using a combination of four or five Gaussian waves in our study [28]. In addition, a Weighted Least Squares (WLS) method is applied to estimate the MG parameters by putting more emphasis on the estimation accuracy of the key points when fitting DVP waveforms without sacrificing the MSE of the estimation.

In comparison with the paper published in IEEE ICIA2011 [28], there are some enhancements as follows:

- The motivation of this paper is fully explained in the introduction.
- The effect of Multi-Gaussian fitting with different number of Gaussians was demonstrated in details, as demonstrated in Section 2.1.
- The proposed algorithm was further described in Section 3.
- The influence of the weight value was further discussed in Section 4.3.
- The four types of pulse waves were changed into five types.
- In this paper, the size of samples has been added into 150 samples, each type of pulse wave including 30 samples.

The paper is organized as follows. The MG model and the corresponding parameter estimation method are introduced in Section 2. The procedure of data acquisition, pulse decomposition and parameter optimization are described in Section 3. In Section 4, a brief discussion on the performance of MG model and the efficacy of WLS is presented. Finally, the conclusion is made in Section 5.

2. Methods

2.1. Multi-Gaussian model

A single-period DVP can be decomposed into forward and backward components as illustrated in Fig. 3. In a pulse waveform, the dicrotic notch, a short time gap related to the backflow, is caused by the closing of the aortic valve [14]. Detailed analysis of DVP waveforms reveals that pulse wave consists of several individual component waves, the first of which is due to the left ventricular ejection from the heart while the remaining component waves are the reflections and re-reflections that originated from the reflection sites [29,30]. Therefore, pulse wave has been considered as the superposition of several Gaussian waves [13–15]. In [14], Rubins et al. tried to describe a DVP waveform as a superposition of four Gaussian waves; while in [15], Martin C. et al. regarded a DVP waveform as a superposition of five individual component waves.

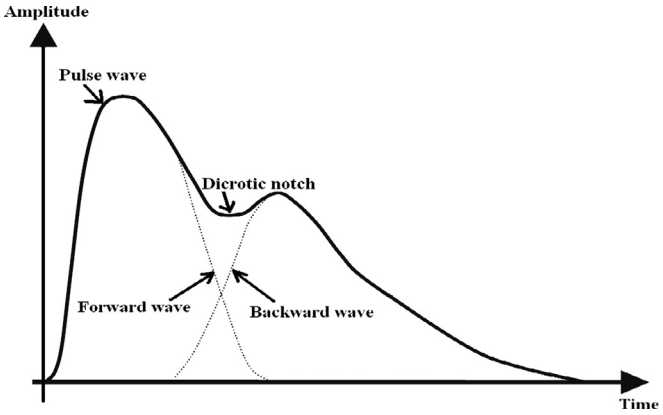

Fig. 3. A pulse wave, its forward and backward waves.

Let $g(t, \Theta)$ represent the discrete version of a 1D Gaussian function, and $\Theta = [H, \mu, \sigma]$ be the unknown parameter vector, $g(t, \Theta)$ is defined as

$$g(t,\Theta) = H \cdot \exp\left(-\frac{(t-\mu)^2}{2\sigma^2}\right) \tag{1}$$

where H is the amplitude of the crest, μ is the time position of the crest, and σ is related to the width of the Gaussian wave. An MG model, denoted as $f_{MG}(t)$, is a sum of Gaussian waves as follows:

$$f_{MG}(t) = \sum_{i=1}^{M} g_i(t,\Theta_i) \tag{2}$$

where, M is the number of the Gaussian waves.

Fig. 4 illustrates a pulse wave and its MG decomposition results using 3–7 Gaussian waves using the MSE criterion, respectively. The percussion wave of pulse wave is asymmetry, which needs to be approximate by two or more Gaussian waves. Therefore, at least three Gaussian waves should be used to approximate a whole single-period pulse wave. The red arrows in Fig. 4(b)–(e) illustrate the effect of increasing the number of Gaussian waves, which demonstrates that using more Gaussian waves can only improve

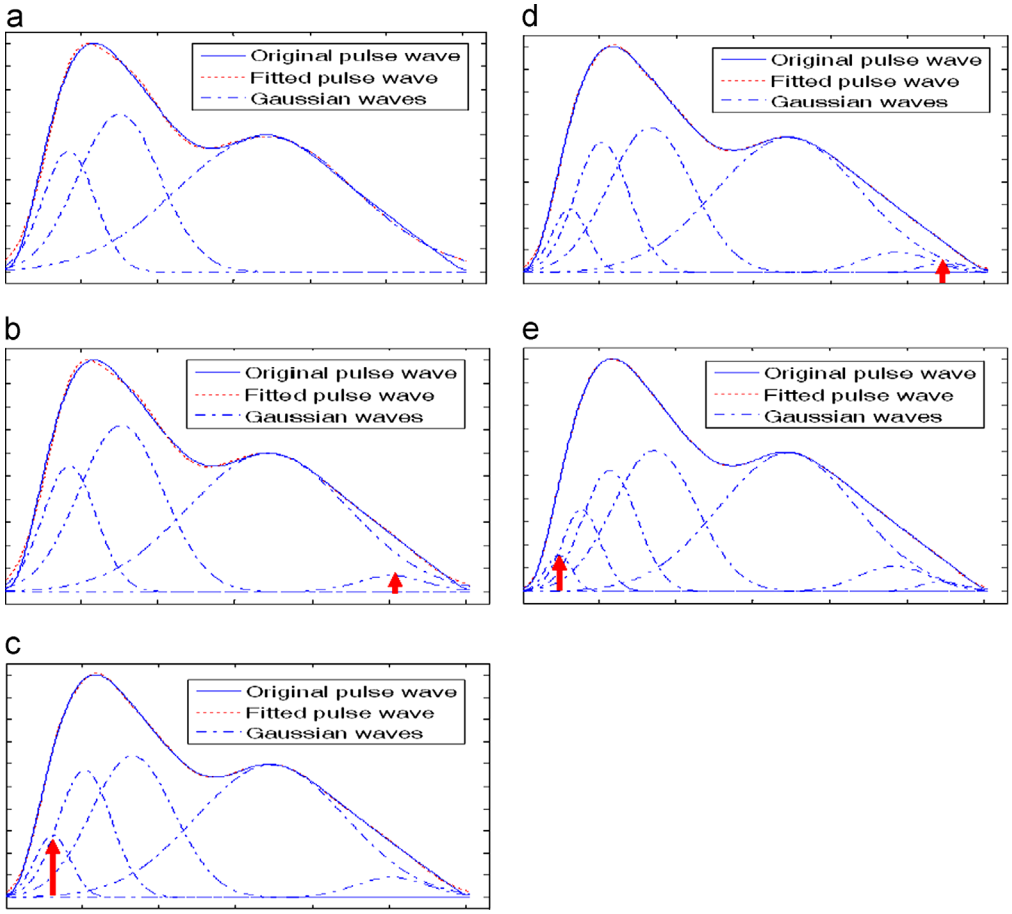

Fig. 4. Pulse wave and its MG decompositions using 3(a), 4(b), 5(c), 6(d), 7(e) Gaussian waves, respectively. (a) Pulse wave and its MG decompositions using three Gaussian waves; (b) Pulse wave and its MG decompositions using four Gaussian waves; (c) Pulse wave and its MG decompositions using five Gaussian waves; (d) Pulse wave and its MG decompositions using six Gaussian waves; (e) Pulse wave and its MG decompositions using seven Gaussian waves. (For interpretation of the references to color in this figure legend, the reader is referred to the web version of this article.)

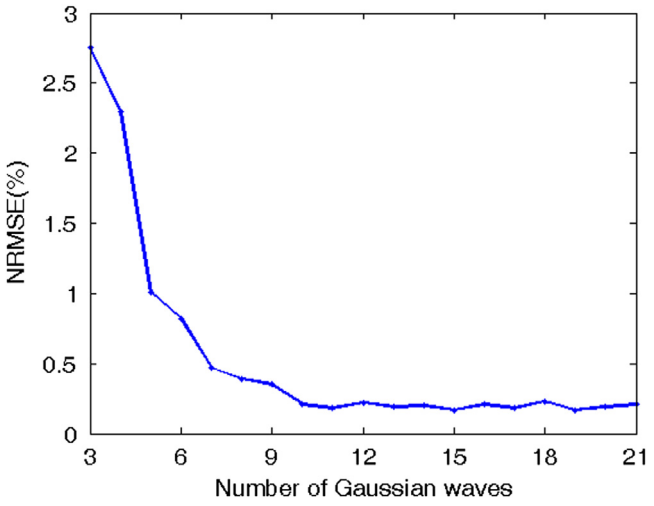

Fig. 5. The NRMSEs of the approximations of the pulse wave in Fig. 4 by using three to twenty-one Gaussian waves.

the accuracy of the approximation in the starting and ending parts of the pulse wave. Fig. 5 shows the Normalized Root Mean Square Error (NRMSE) of the approximations of the pulse wave in Fig. 4 by using three to twenty-one Gaussian model fitting methods.

The diagnosis from pulse wave is similar to that from ECG [31]. In the digital signal processing of ECG, Gavin P. Shorten et al. used the total percentage root-mean square difference (PRD) as the criterion to evaluate the performance of the ECG compression algorithms. They set 2.5% as the acceptable PRD for ECG compression [32]. To quantify the performance of the MG decomposition method, we proposed three parameters, namely Errx, Erry and NRMSE. The related report on the acceptable threshold for the evaluation criterion for decomposing pulse wave has not been found. The parameter NRMSE is similar to the PRD of ECG signal. Here, we set the acceptable threshold of NRMSE as 2%. For the pulse wave illustrated in Fig. 4, five Gaussian waves are enough to approximate at the accuracy of NRMSE being less than 2% [31,32]. The least number of Gaussian waves needs to be selected within the required decomposition accuracy for the convenience of pulse wave compressing and analysis. Therefore, an adaptive MG model is proposed in this paper to approximate DVP waveform with the least number of Gaussian waves (the DVP signals that we have processed are fitted by 4 or 5 Gaussian waves) within the boundaries of the acceptable NRMSE.

2.2. Estimation of the MG model parameters for approximating pulse wave

The proposed adaptive MG model describes the DVP waveform as a sum of 4 or 5 Gaussian waves, with each pulse being determined by the corresponding parameter vector $\Theta_i = [H_i, \mu_i, \sigma_i]$. Therefore, 12–15 parameters need to be estimated in the model. The Nonlinear Least Squares (NLS) method has usually been used for curve fitting, assuming that each observation in the data set to be fitted has equal importance [33]. However, some morphological features in pulse waves are more important for diagnosis, e.g. some key points such as the crests and troughs of pulse wave. The estimation error of these points should be small enough for correct diagnosis.

In this paper, the WLS method is used to estimate parameters in the MG model because the positions of sampling points in DVP have different degrees of importance. The best fit in the WLS method minimizes the weighted sum of squared residuals, and the weight determines how much each observation in the data set influences the final parameter estimation [33]. The WLS criterion for the MG model is that the model is optimal when the weighted sum of the squared residuals Q defined in formula (3) is the minimum.

$$Q = \sum_{i=1}^{N} w_i [y_i - f_{MG}(x_i, \Theta)]^2 \quad (3)$$

where (x_i, y_i) is the time position and amplitude of the ith sampling point, Θ is the vector of unknown parameters and w_i is the weight of the ith sampling point.

To find the value of Θ which minimizes Q in the Eq. (3), the Levenberg–Marquardt Algorithm (LMA), an iterative numerical algorithm, is applied. LMA interpolates between Gauss–Newton Algorithm (GNA) and Gradient Descent Method (GDM). In comparison to GDM and GNA, LMA is more robust [34]. First, LMA can be used to find an acceptable solution even if the initial parameters start very far from the final minimum. Second, the second order derivative or Hessian of the squared error over a window is used to avoid any shallow region of the error surface once it is close to the minima. Third, a faster convergence within a few cycles following a large disturbance can be achieved.

LMA has good performance in the optimization procedure. When the current solution is far from the optimized solution, the algorithm behaves like the steepest descent method: slow, but guaranteed to converge. When the current solution is close to the optimized solution, it becomes a GNA [34]. Like most numerical algorithms, LMA involves selecting initial values for the parameters. Then, the parameters are refined iteratively till the max iteration is reached or the termination conditions are matched. The estimation of initial values will be introduced in Section 3.

3. Pulse decomposition and parameter optimization

Fig. 6 illustrates our proposed MG pulse wave approximation method that combines WLS and Multi-Criteria Decision Making (MCDM). In this proposed approach, the noise and baseline wander of pulse wave is removed firstly [35]; then the single-period pulse wave is segmented from the processed pulse wave and fitted using 4-Gaussian model with different weights. Having employed the multi-criteria decision making strategy to optimize the weights for the corresponding points of pulse wave, the accuracy of the fitting will be calculated. If the accuracy is with in the 2%, the decomposition will be ended; otherwise, the 5-Gaussian model will be employed.

3.1. Data acquisition and preprocessing

DVP signals were collected from 800 volunteers (500 young health students at the age of 20–25, 300 patients at the age of 30–80) using a pulse sensor fixed on the left index finger in a sitting position under controlled environmental condition. Before the measurements, the volunteers were asked to relax in a sitting position for 3 min. The duration of measurement was between 120 s and 150 s. The signals were sampled at 1 kHz.

The collected DVP signals were processed offline by our proposed method implemented using MATLAB. At first, data sets were preprocessed, including the removal of the direct component and baseline wander component (0–0.1 Hz) by a wavelet-based cascaded adaptive filter (CAF) [36], removal of random noise ($>$ 15 Hz) by a Savitsky–Golay smoothing filter and detection of all feet of DVPs. Then, the DVP for each heartbeat period was normalized.

3.2. The decomposition of pulse waves

DVP is classified into four classes by Dawber's analysis on DVP from 1778 individuals in 1965 and 1966 [37]. In this paper, the four types defined by Dawber et al. were reclassified into five types,

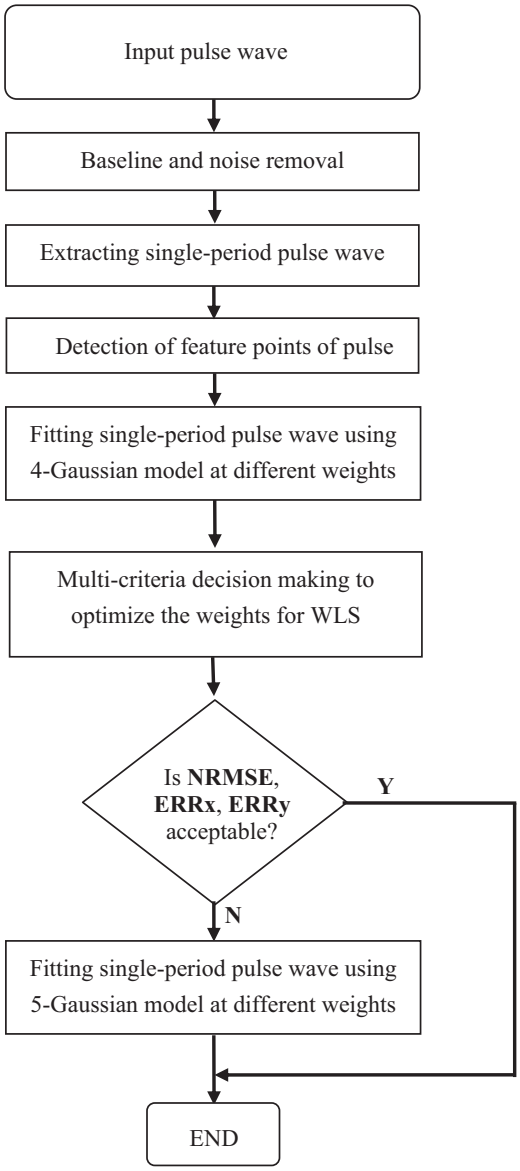

Fig. 6. The flow chart of the proposed MG modeling method combining the WLS and MCDM methods.

where the third type was divided into two types. The class 3 with bisferiens was divided into the fourth type. Fig. 7 demonstrates DVP waveforms with different types. To evaluate the performance of the MG model on different DVP waveforms morphologically, we selected 150 pulse data whose signal-to-noise ratio is higher than 20 dB from our pulse database for the study (30 pulse data for each type of DVP).

It is also mentioned that a direct wave and a reflected wave appears in the forward part of a single-period DVP [14]. Therefore, in our calculation, we assume that a part of the reflected wave also appears in the forward part and two or three reflected waves constitute the backward part in a single-period DVP. In summary, one direct wave and three or four reflected waves were considered in the MG decomposition of pulse waves.

The vector parameter $\Theta=[H,\ \mu,\ \sigma]$ of each decomposed Gaussian wave is estimated by the amplitude (A_i) and the duration position (D_i) of feature points P_i ($i=1, \ldots, 4$), as shown in Fig. 8, and P_i is extracted by the double differentiation method combined with our estimation. According to [10,38,39], the positions of the crests of direct wave and the reflected waves of single-period DVP

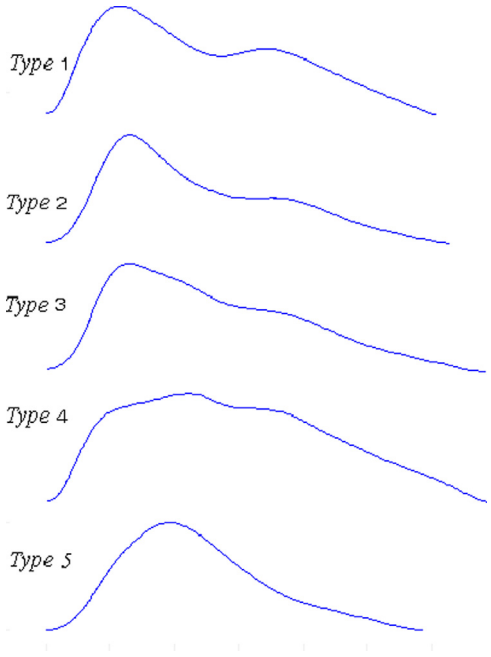

Fig. 7. Five types of DVP waveforms [26,31]. Type 1: Distinct notch is notable on the downward slope of the pulse wave. Type 2: No notch develops but the line of descent becomes horizontal. Type 3: No notch develops but there is a well-defined change in the angle of the descent. Type 4: No notch develops but there is a notable reflecting wave in the systolic component of the pulse wave, with bisferiens in the ascending segment of the pulse wave. Type 5: No notch develops or no change occurs in the angle of descent.

can be determined by the positions of typical waves defined in Fig. 2(a) and the zero crossing points of the SDDVP.

In this paper, a single-period DVP is first fitted by a 4-Gaussian MG model, and then a 5-Gaussian MG is used when the 4-Gaussian MG cannot meet our criterion (NRMSE < 2%, Errx < 6 ms, Erry < 0.01). The estimation of the duration D_1, D_2, D_3, and D_4 is specified in detail as follows:

D_1: The x-axis position of the first trough of the SDDVP for all types.
D_2: The x-axis position of the SDDVP's first crest after $P1$.
The first zero-crossing point of the SDDVP is selected if a crest does not exist before dicrotic notch (the first type and the second type) or 0.5T* (the third type, fourth type and the fifth type).
D_3: The x-axis position of the second crest of DVP for the first type; the position of the first zero-crossing point of the SDDVP after the dicrotic notch for the second, third and fourth types; the position of the first zero-crossing point in the time interval 0.4–0.5 T for the fifth type.
D_4: The medial x-axis position between $P3$ and the ending point.

*T is the period of DVP.

When the duration positions of the feature points are determined, the initial parameters of the decomposed Gaussian waves in the MG model can be estimated. Table 1 lists the initial values of μ, H and σ of 4-Gaussian model for decomposition. Fig. 8 shows the estimation results of the feature points (Fig. 8(a1)–(e1)) and the decomposed Gaussian waves for five types of DVP (Fig. 8(a2)–(e2)).

3.3. Parameter optimization using multi-criteria decision making

Let $f_{DVP}(n)$, $0 < n < N$, denote an amplitude-normalized, time-averaged single-cycle DVP derived from the processed DVP signals, where 'N' is the number of data points contained in $f_{DVP}(n)$.

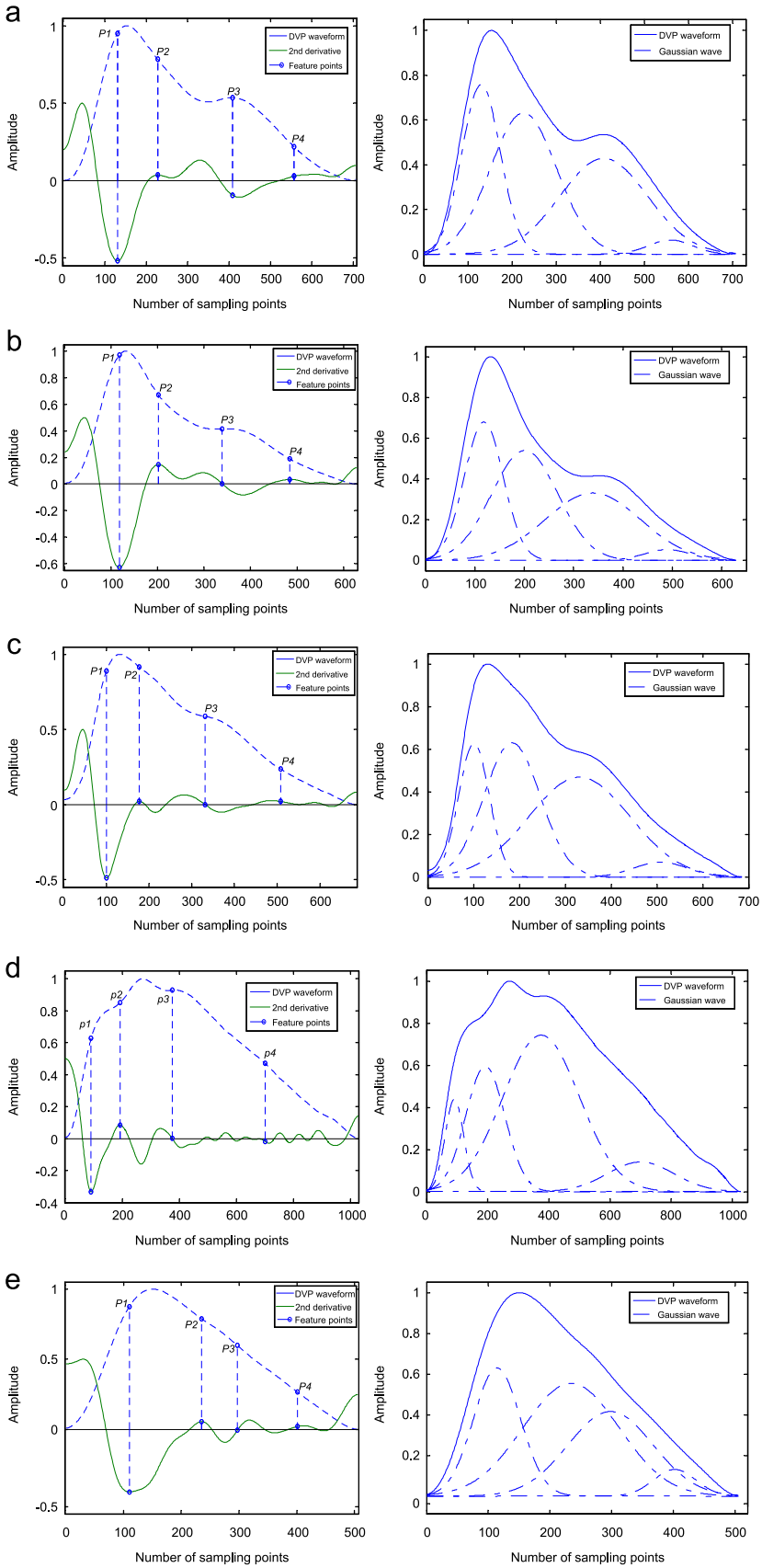

Fig. 8. The five types of DVPs, their second derivatives, feature points, and corresponding decomposed Gaussian waves. (a1) The Type 1 DVP, its second derivative and the estimation of feature points; (a2) The Type 1 DVP and its four decomposed Gaussian waves; (b1) The Type 2 DVP, its second derivative and the estimation of feature points; (b2) The Type 2 DVP and its four decomposed Gaussian waves; (c1) The Type 3 DVP, its second derivative and the estimation of feature points; (c2) The Type 3 DVP and its four decomposed Gaussian waves; (d1) The Type 4 DVP, its second derivative and the estimation of feature points; (d2) The Type 4 DVP and its four decomposed Gaussian waves; (e1) The Type 5 DVP, its second derivative and the estimation of feature points; (e2) The Type 5 DVP and its four decomposed Gaussian waves; The (a1), (b1), (c1), (d1), and (e1) are rough estimation results of feature points; (a2), (b2), (c2), (d2), and (e2) are decomposed Gaussian waves.

Table 1
Initial estimation of μ, H and σ.

Parameter	H_i					μ_i	σ_i				
DVP type	1	2	3	4	5	1–5	1	2	3	4	5
$i=1$	$0.8A_1$	$0.7A_1$	$0.7A_1$	$0.7A_1$	D_1	$D_1/3$					
$i=2$	$0.8A_2$	$0.8A_2$	$0.7A_2$	$0.7A_2$	D_2	$(D_2-D_1)/3$	$D_2/3$				
$i=3$	$0.8A_3$	$0.8A_3$	$0.8A_3$	$0.7A_3$	D_3	$min((T-D_3),D_3)/3$					
$i=4$	$0.3A_4$	$0.3A_4$	$0.3A_4$	$0.5A_4$	D_4	$(T-D_4)/3$					

Table 2
Fitted results of five types of pulse wave using MG model.

	Type 1	Type 2	Type 3	Type 4	Type 5	Total
4-MG model	12	26	28	21	30	117
5-MG model	18	4	2	9	0	33

According to WLS, the parameters of the MG model are evaluated by minimizing the following sum:

$$\mathrm{MSE}=\frac{1}{N}\sum_{n=1}^{N}\frac{w_n}{W}[f_{DVP}(n)-f_{MG}(n,\Theta)]^2,\quad W=\sum_{n=1}^{N}w_n \tag{4}$$

In this paper, NRMSE is calculated to evaluate the accuracy of the MG model and is used to compare the fitted results with the original ones.

$$\%\ \mathrm{NRMSE}=\sqrt{\frac{\sum_{n=1}^{N}w_n[f_{DVP}(n)-f_{MG}(n,\Theta)]^2}{\sum_{n=1}^{N}w_n f_{DVP}(n)^2}}\times 100\% \tag{5}$$

where, $f_{DVP}(n)$ is fitted by $f_{MG}(n,\Theta)$ through solving formula (4), w_n is the weight corresponding to the nth point, W is the sum of the weight vector. The unknown parameter vector Θ in $f_{MG}(n,\Theta)$ are determined by minimizing the MSE in formula (4) using LMA. Initial values of the unknown parameters in LMA are provided by the estimation in Table 1.

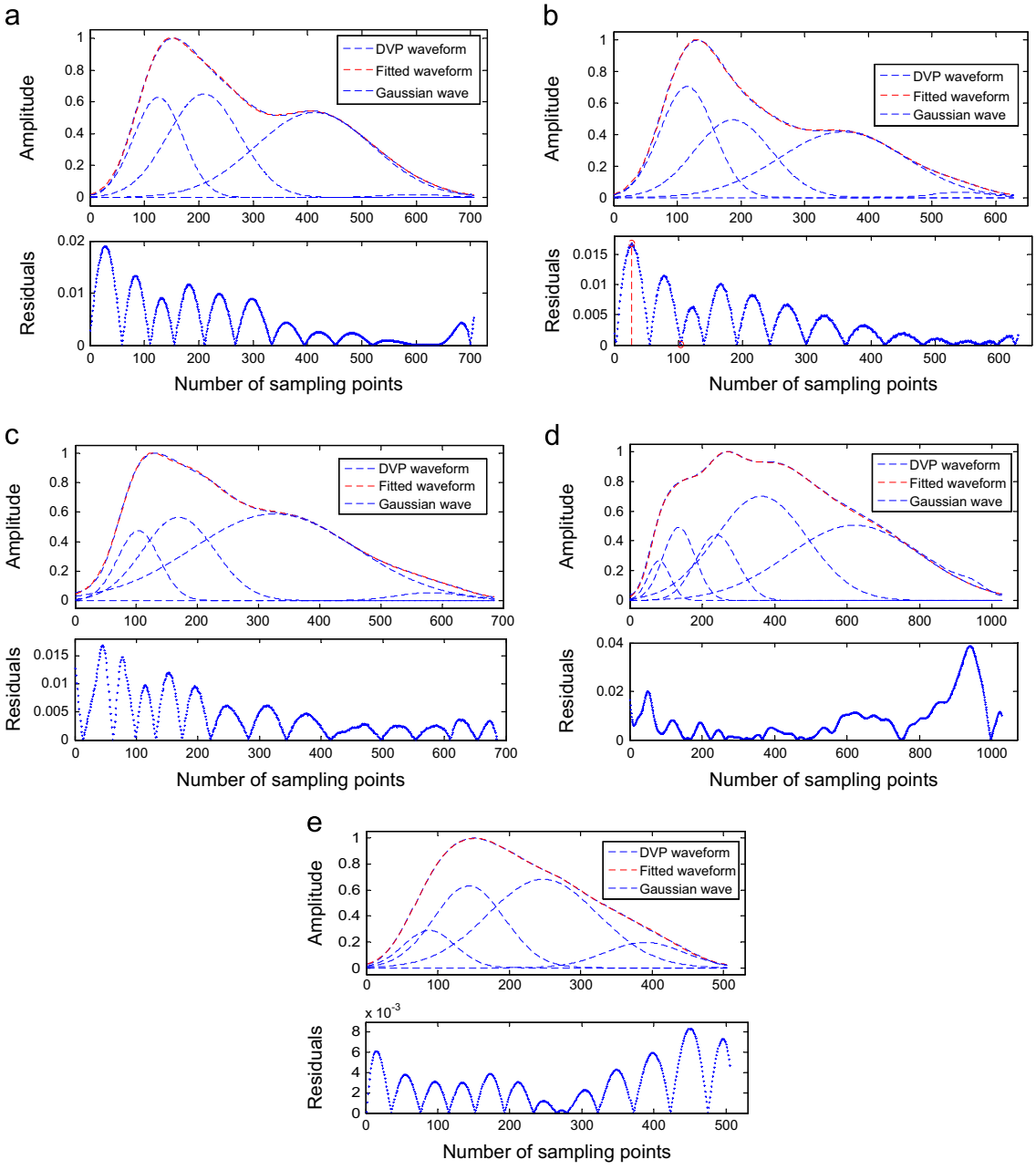

Fig. 9. DVP waveform fitted by 4-Gaussian MG model in (a), (b), (c), (e) and by 5-Gaussian MG model in (d).

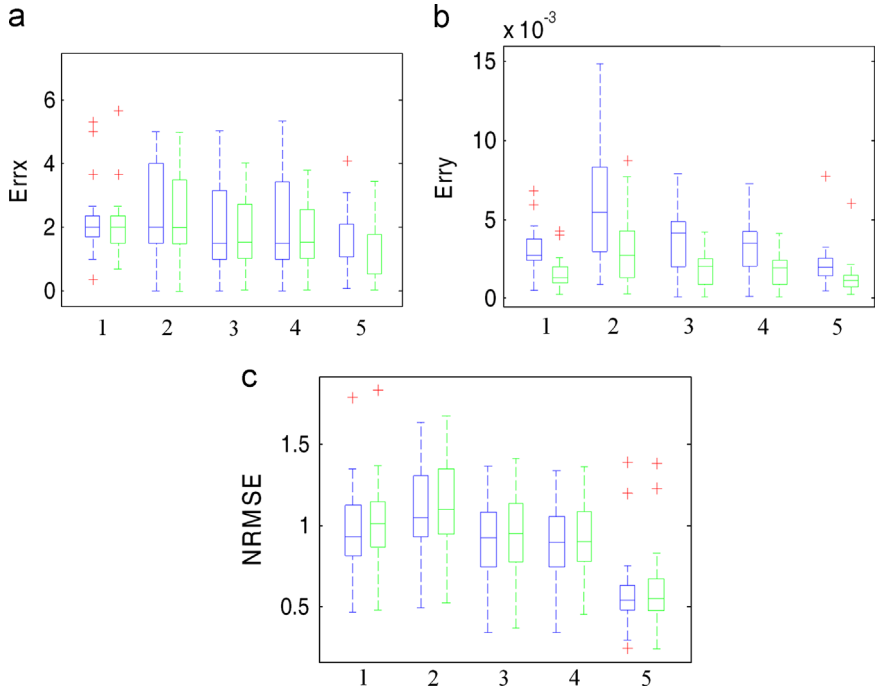

Fig. 10. Box plot of MG model's criteria Errx, Erry and NRMSE for 150 data sets (30 data sets for each type). Numbers on *x*-axis represent DVP types. Blue box and green box represent criteria values of NLS and WLS, respectively. (For interpretation of the references to color in this figure legend, the reader is referred to the web version of this article.)

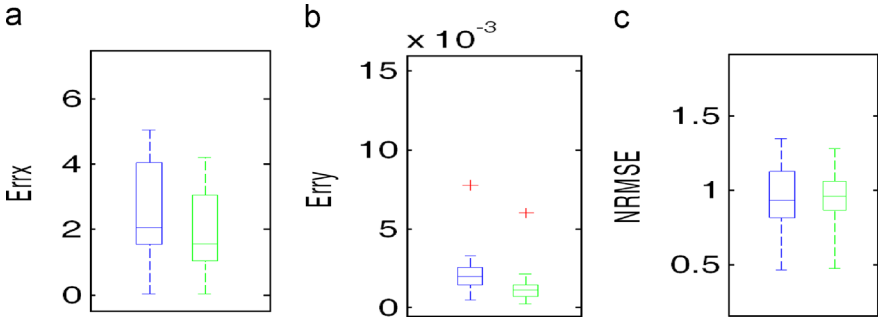

Fig. 11. Box plot of MG model's criteria Errx, Erry and NRMSE for a volunteer"s pulse wave with 100 continuous periods. Blue box and green box represent criteria values of NLS and WLS method respectively. (For interpretation of the references to color in this figure legend, the reader is referred to the web version of this article.)

In order to find the best weight values to minimize the absolute-error of key points selected in Section 2 with a limitation of MSE, a group of 100 different w was tested. In this group, w corresponding to important points changes from one to one hundred by step one, while the w corresponding to the other points maintains a value of one. Furthermore, a hundred fitted results corresponding to different weight values will be evaluated by criteria **Errx**, **Erry**, and **NRMSE**.

Errx—sum of absolute errors of x-axis positions between crests and troughs in $f_{MG}(n,\Theta)$ and $f_{DVP}(n)$.
Erry—sum of absolute errors of amplitudes between crests and troughs in $f_{MG}(n,\Theta)$ and $f_{DVP}(n)$.

As criteria NRMSE, Errx, and Erry may conflict with each other, finding the best weight vector can be regarded as a MCDM problem. The preferences in the MCDM theory may be formulated and expressed in a cardinal vector of normalized criterion preference weights. Consider Errx, Erry, NRMSE as $a_{.1}$, $a_{.2}$, $a_{.3}$ and the fitted results as set $F=\{f_1, f_2, \ldots, f_i, \ldots, f_{100}\}$ (f_i represents result corresponding to the ith weight vector) [40]. The optimal weight is decided according to the decision making theory [41] by the following steps:

Step 1: Setting up a decision matrix.
There are 100 results to be assessed for each of the three criteria, $a_{.1}$, $a_{.2}$, $a_{.3}$. Therefore, the decision matrix is a 100×3 matrix with each element r_{ij} ($1\le i\le 100$, $1\le j\le 3$) corresponding to the jth criteria value of the ith fitting result. As $a_{.1}$, $a_{.2}$, $a_{.3}$ are cost criteria, r_{ij} is calculated by the following formula [34]:

$$r_{ij}=\frac{\max(a_{\cdot j})-a_{ij}}{\max(a_{\cdot j})-\min(a_{\cdot j})}, \tag{6}$$

where, $max(a_j)$ and $min(a_j)$ are the maximum and minimum value of a_j, respectively.
Criteria $a_{.1}$, $a_{.2}$, $a_{.3}$ are normalized by this formula to make sure $0\le r_{ij}\le 1$.
Step 2: Setting relative weight value u_j for criterion a_j.
Relative weight value is normalized ($u_1+u_2+u_3=1$ and $0\le u_j\le 1$) and decided by the relative importance of criteria.

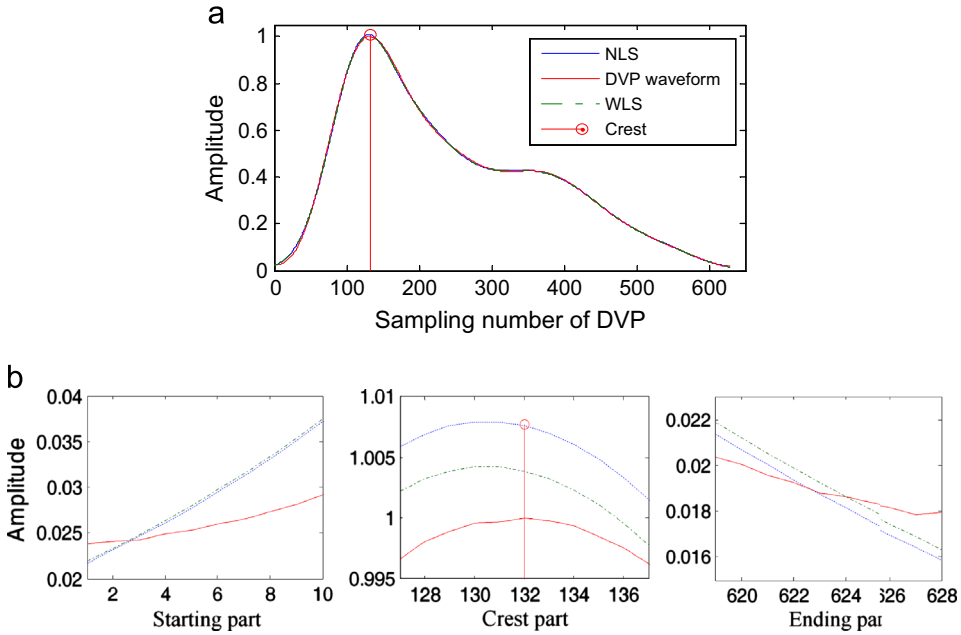

Fig. 12. (a) A single-period DVP and MG model achieved by NLS and WLS and (b) local enlargement of the ascending segment, crest segment, descending segment of waveform in (a).

To minimize Errx and Erry with the limitation of NRMSE, we set $u_1=u_2=0.35$, $u_3=0.3$ according to trials and errors.

Step 3: Calculating the fitness value c_i for each f_i in set F.

In this step, an extreme optimal solution E and an extreme bad solution B are defined as: $E=(e_1, e_2, e_3)$, $B=(b_1, b_2, b_3)$, where $e_j=max(r_{.j})$, $b_j= min(r_{.j})$ [42]. It is obvious in this case that $E=(1, 1, 1)$, $B=(0, 0, 0)$. E is an ideal solution that is nonexistent under general conditions in the MCDM problem. In this paper, the best solution is obtained by calculating the fitness value c_i for each f_i as follows:

$$c_i = \frac{1}{1+\left(\sum_{j=1}^{3}[u_j(e_j-r_{ij})]^2 / \sum_{j=1}^{3}[u_j(b_j-r_{ij})]^2\right)} \tag{7}$$

A fitness value set $C=\{c_1, c_2, \ldots, c_i, \ldots, c_{100}\}$ is obtained for $F=\{f_1, f_2, \ldots, f_i, \ldots, f_{100}\}$.

Step 4: Finding the best solution.

The result f_i that corresponds to the maximum fitness value c_i is taken as the best solution.

4. Results and discussions

4.1. Performance of MG modeling

A total of 150 DVP signals were processed and fitted by the MG Model, 117 and 33 of which are fitted by 4-Gaussian MG and 5-Gaussian MG, respectively. Table 2 shows that 5-Gaussian MG is used more frequently in the first type than in other types of DVP waveforms; 4-Gaussian MG can be applied to approximate all the fifth type DVP waveforms in this study.

The fitted results of the five single-period DVPs illustrated in Fig. 8 are shown in Fig. 9. Though DVP waveforms of different types show differences in morphology; they are all well fitted by the MG model. In general conditions, the residuals between the normalized DVP waveform and the fitted MG model did not exceed 2%, except for the 20–40th sampling points after the starting point and 10–30th sampling points before the ending point of a single-period DVP.

The degraded performance of MG model at the starting and ending part of DVP is mainly due to two reasons. First, the ascending and descending parts of a Gaussian wave and a DVP waveform have different gradient variation tendencies. To guarantee the agreement between the MG model and the DVP waveform around the crest segment, the accuracy of the fitting in other parts cannot be achieved. Second, a small wave may exist at the ending part of a DVP waveform, especially when the descending segment after dicrotic notch is very long (exceeding the half of the DVP period).

4.2. Comparison between the NLS and the WLS

Performances of the NLS and the WLS are compared using the evaluation criteria Errx, Erry, NRMSE of the MG model. Fig. 10 shows the statistical results of the fitted 150 DVP waveforms. It is notable that the MG model obtained by the WLS has better performance than that by the NLS method in Erry and Errx. The deviations of the positions (in time and amplitude) of the key points obtained by the WLS method are smaller compared to those obtained by the NLS method. However, at the same time, the mean NRMSE of WLS is slightly higher than that of NLS, because residuals on ordinary points (weighted by the value of one) are increased, when the WLS method optimizes parameters by putting more emphasis on reducing residuals on important points (weighted by the optimized value). Fig. 11 illustrates the statistical results of a volunteer's pulse wave for 100 continuous periods. It is notable that the MG model obtained by WLS has a much better performance than that by NLS method in Erry and Errx, which means that the WLS method is more precise because the standard deviation of parameters obtained by WLS is smaller than that by the NLS.

In Fig. 12, results of fitting a DVP waveform with the MG model by the WLS and the NLS algorithms at the starting, the ending and the crest segments are compared. From these figures it can be seen that the WLS performs better than the NLS at the area near the crest of the DVP waveform.

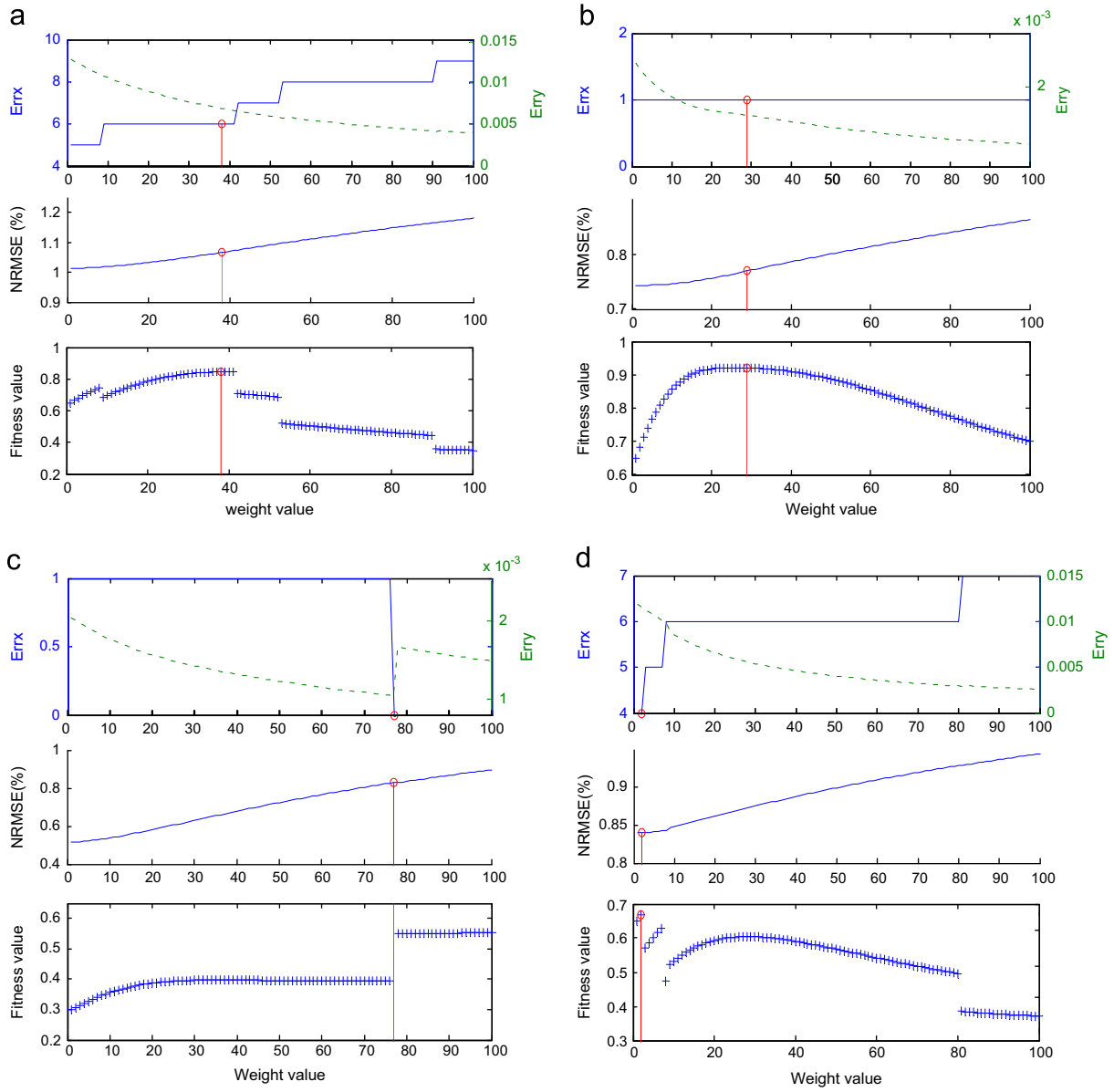

Fig. 13. Change of Errx, Erry, NRMSE and FV* with varying WV* in four situations. (a). Best FV exists in the range 10 through 40 with a crest. FV changes discontinuously. (b). Best FV exists in the range 10 through 40 with a crest. FV changes continuously. (c). Best FV exists in the range 40 through 90. FV may suddenly increase when Errx decreased. (d). Best FV exists in the range 1 through 10. FV may start to decrease with a small WV.*FV – fitness value, WV – weight values on important points.

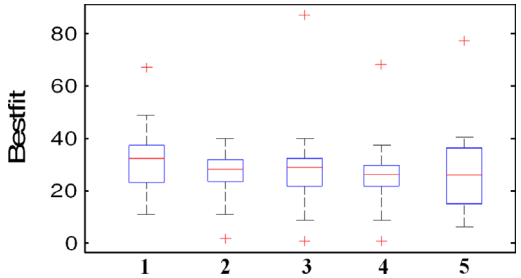

Fig. 14. Result of best fitted weight value. Numbers on *x*-axis represent DVP types.

4.3. *Influences of the weight value*

In Section 3, 100 different w were tested using the WLS algorithm to find the optimized weight vector. The criteria Errx, Erry, NRMSE were used in the MCDM method. With the increment of the weight values of important points, the fitness value changed in different ways. Fig. 13 shows four different situations.

Fig. 13(a) illustrates a common situation: when increasing the weight value on key points, Erry always decrease continuously; Errx always increase discontinuously because the MG model may be over weighted; NRMSE always increases, but its variation range does not exceed 0.3%; The best fitness values always occur at the range from 20 to 40. However, as Fig. 13(b), (c), (d) illustrated, exceptional cases do exist. In Fig. 13(b), (c), Errx does not change or even decrease in several DVP waveforms of the fourth type. Due to the sudden changes in Errx, in Fig. 10(c), an abrupt slope occurs in Erry. In Fig. 13(c), (d), the optimal fitness values occur in the range greater than 50 and less than 10, respectively.

Fig. 14 demonstrates the result of the best weights corresponding to the best fitness of the five types of pulse waves, which indicates that the MG model performs well when the weight value on important points lies between 20 and 40, while the best weights for different types of DVP differ slightly.

5. Conclusions

The decomposition analysis method is effective in compressing, synthesizing and analyzing physiological signals. There are some reported researches that decompose physiological signals using multiple Gaussian models. However, the number of Gaussian wave is constant. Actually, the number of Gaussian waves depends on the morphology of physiological signals. Furthermore, those methods do not pay much attention to the estimation error of the key points in physiological signals. In fact, the positions of these key points are important for diagnosis.

To analyze component waves in five types of DVP waveforms, an adaptive MG model is introduced in this paper. The model closely approximates a single-period DVP by decomposing it into four or five Gaussian waves. When applying the MG model to 150 DVP waveforms of five different types, it performed well (NRMSE $<2\%$, Errx <6 ms, Erry <0.01). It should be noted that the choice between 4-MG and 5-MG model is determined by the morphology of the DVP waveform.

The parameters of the MG model are estimated by the Double Differentiation method first and then optimized by WLS. Due to the crests and troughs of DVP waveforms contain clinical information, the fitted residual error of those points' amplitudes and positions are required to be smaller by means of assigning the larger weights to them in WLS. In Section 4, the analysis demonstrated that WLS is superior to NLS, because the agreement of the MG model achieved by WLS is better than that by NLS at the crests and troughs of DVP waveforms.

In order to find the set of weight values in the WLS method that can obtain the best fitting performance of MG model to DVP waveform, a group of 100 different weight vectors were tested in Section 3. The MCDM method was applied to choose the best weight vector by three criteria, namely NRMSE, Errx and Erry. Experimental results show that the MG model always performs well when the weight value for key points lies between 20 and 40.

Component waves of the MG model may relate to the forward and reflected waves in a single-period DVP. As information of the forward and reflected waves are useful in arterial parameter estimation, further research on amplitude and position estimation of the component Gaussian waves are possibly of great significance to the advancement in arterial parameter estimation. This proposed approach also can be applied to decompose the other related physiological signals.

Conflict of interest statement

We declare that we have no financial and personal relationships with other people or organizations that can inappropriately influence our work, there is no professional or other personal interest of any nature or kind in any product, service and/or company that could be construed as influencing the position presented in, or the review of, the manuscript entitled, “Multi-Gaussian Fitting for Pulse Waveform Using Weighted Least Squares and Multi-Criteria Decision Making Method”.

Acknowledgments

This work is supported by the National Natural Science Foundation of China (No. 61374015), the Ph.D. Programs Foundation of Ministry of Education of China (No. 20110042120037), the Liaoning Provincial Natural Science Foundation of China (No. 201102067) and the Fundamental Research Funds for the Central Universities (No. N110219001). This work is also supported in part by the Hong Kong Research Grants Council (RGC) General Research Fund (No. 415709).

References

[1] J. Spigulis, Optical non-invasive monitoring of skin blood pulsations, Appl. Opt. 44 (10) (2005) 1850–1857.
[2] J. Allen, A. Murray, Age-related changes in the characteristics of the photoplethysmographic pulse shape at various body sites, Physiol. Meas. 24 (2) (2003) 297–307.
[3] J. Allen, Photoplethysmography and its application in clinical physiological measurement, Physiol. Meas. 28 (2007) R1–R39.
[4] D. Goswami, K. Chaudhuri, J. Mukherjee, A new two-pulse synthesis model for digital volume pulse signal analysis, Cardiovasc. Eng. 10 (3) (2010) 109–117.
[5] Bing Nan Li, Bin Bin Fu, Ming Chui Dong, Development of a mobile pulse waveform analyzer for cardiovascular health monitoring, Comput. Biol. Med. 38 (4) (2008) 438–445.
[6] Yu-Feng Chung, Chung-Shing Hu, Cheng-Chang Yeh, Ching-Hsing Luo, How to standardize the pulse-taking method of traditional Chinese medicine pulse diagnosis, Comput. Biol. Med. 43 (4) (2013) 342–349.
[7] Ching-Chuan Wei, Chin-Ming Huang, Yin-Tzu Liao, The exponential decay characteristic of the spectral distribution of blood pressure wave in radial artery, Comput. Biol. Med. 39 (5) (2009) 453–459.
[8] Wilmer W. Nichols, Michael F. O'Rourke, Charalambos Vlachopoulos, McDonald's Blood Flow in Arteries: Theoretical, Experimental and Clinical Principles, 6th Edition, CRC Press, 2011.
[9] H.B. Grotenhuis, J.M. Westenberg, P. Steendijk, R.J. Van der Geest, et al., Validation and reproducibility of aortic pulse wave velocity as assessed with velocity-encoded MRI, J. Magn. Reson. Imaging. 30 (3) (2009) 521–526.
[10] K. Takazawa, N Tanaka, M. Fujita, et al., Assessment of vascoactive agents and vascular aging by the second derivative of photoplethysmogram waveform, Hypertension 32 (2) (1998) 365–370.
[11] I. Imanaga, H. Hara, S. Koyanagi, et al., Correlation between wave components of the second derivative of the plethysmogram and arterial distensibility, Jpn. Heart J. 39 (6) (1998) 775–784.
[12] L.A. Bortolotto, J. Blacher, T. Kondo, et al., Assessment of vascular aging and atherosclerosis in hypertensive subjects: second derivative of photoplethysmogram versus pulse wave velocity, Am. J. Hypertension 13 (2) (2000) 165–171.
[13] Weili Qian, Lanyi Xu, Fuyu Chen, Rongliang Zheng, Acquiring characteristics of pulse wave by Gaussian function separation, Chin. J. Biomed. Eng. 13 (1) (1994) 1–7.
[14] Uldis Rubins, Finger and ear photoplethysmogram waveform analysis by fitting with Gaussians, Med. Biol. Eng. Comput. 46 (12) (2008) 1271–1276.
[15] M.C. Baruch, D.ER Warburton, S.SD Bredin, et al., Pulse decomposition analysis of the digital arterial pulse during hemorrhage simulation, Nonlinear Biomed. Phys. 5 (1) (2011).
[16] Berend E. Westerhof, Ilja Guelen, et al., Quantification of wave reflection in the human aorta from pressure alone: a proof of principle, Hypertension 48 (4) (2006) 595–601.
[17] C. Gillebert, L.M.V. Bortel, S. Patrick, et al., Evaluation of noninvasive methods to assess wave reflection and pulse transit time from the pressure waveform alone, Hypertension 53 (2009) 142–149.
[18] R. Couceiro, P. Carvalho, R.P. Paiva, J. Henriques, M. Antunes, I. Quintal, J. Muehlsteff, Multi-Gaussian fitting for the assessment of left ventricular ejection time from the photoplethysmogram, in: Proceedings of the International Conference of the IEEE Engineering in Medicine and Biology Society, EMBC 2012, San Diego, USA.
[19] S. Mohanalakshmi, A. Sivasubramanian, A review on the non-invasive assessment of atherosclerosis and other cardiovascular risk factors through the second derivative of the photoplethysmogram (SDPPG), Int. J. Syst., Algor. Appl. 2 (ICRASE12) (2012) 166–170.
[20] Yinghui Chen, Lei Zhang, David Zhang, Dongyu Zhang, Wrist pulse signal diagnosis using modified Gaussian models and Fuzzy C-Means classification, Med. Eng. Phys. (2009) 1283–1289.
[21] P.J. Chowienczyk, R.P. Kelly, Helen MacCallum, et al., Photoplethysmographic assessment of pulse wave reflection, J. Am. Coll. Cardiol. 34 (7) (1999) 2007–2014.
[22] S.C. Millasseau, F.G. Guigui, R.P. Kelly, et al., Non-invasive assessment of the digital volume pulse: comparison with the peripheral pressure pulse, Hypertension 36 (2000) 952–956.
[23] Bernhard Hametnera, Siegfried Wassertheurer, Johannes Kropf, Christopher Mayer, Andreas Holzinger, Bernd Eber, Thomas Weber, Wave reflection quantification based on pressure waveforms alone-methods, comparison, and clinical covariates, Comput. Methods Programs Biomed. 109 (2013) 250–259.
[24] Matti Huotari, Antti Vehkaoja, Kari Määttä, Juha Kostamovaara, Photoplethysmography and its detailed pulse waveform analysis for arterial stiffness, J. Struct. Mech. 44 (4) (2011) 345–362.
[25] Matti Huotari, Antti Vehkaoja, Kari Määttä, Juha Kostamovaaraa, Pulse waveforms are an indicator of the condition of vascular system, IFMBE Proceedings of the World Congress on Medical Physics and Biomedical Engineering 39 (2013) 526–529.
[26] Chengyu Liu, Dingchang Zheng, Alan Murray, Changchun Liu, Modeling carotid and radial artery pulse pressure waveforms by curve fitting with Gaussian functions, Biomed. Signal. Process Control (2013) 449–454.

[27] Y. Zhao, W.H. Kullmann, Applanation tonometry for determining arterial stiffness, Biomed. Tech. 57 (Suppl.1) (2012) 669–672.
[28] Lisheng Xu, Shuting Feng, Yue Zhong, Cong Feng, Max Q.-H. Meng, Huaicheng Yan, Multi-Gaussian fitting for digital volume pulse using weighted least squares method," in: Proceedings of IEEE International Conference on Information and Automation (ICIA2011), Shenzhen China, June 6–8, 2011, pp. 544–549.
[29] S.C. Millaseau, R.P. Kelly, J.M. Ritter, et al., Determination of age-related increases in large artery stiffness by digital pulse contour analysis, Clin. Sci. 103 (4) (2002) 371–377.
[30] S.C. Millaseau, J.M. Ritter, K. Takazawa, Contour analysis of the photoplethysmographic pulse measured at the finger, J. Hypertension 24 (8) (2006) 1449–1456.
[31] Gang Zheng, Qingjun Huang, Guodong Yan, Min Dai, Pulse waveform key point recognition by wavelet transform for central aortic blood pressure estimation, J. Inf. Comput. Sci. 9 (1) (2012) 25–33.
[32] Gavin P. Shorten, Martin J. Burke, The application of dynamic time warping to measure the accuracy of ECG compression, Int. J. Circuits, Syst. Signal Process. 5 (3) (2011) 305–313.
[33] N. Cressie, Fitting variogram models by weighted least squares, Math. Geol. 17 (5) (1985) 563–585.
[34] M.T. Hagan, H.B. Demuth, M.H. Beale, Neural Network Design, PWS Pub, Boston, London, 1996.
[35] Jung Kim Hyonyoung Han, Artifacts in wearable photoplethysmographs during daily life motions and their reduction with least mean square based active noise cancellation method, Comput. Biol. Med. 42 (4) (2012) 387–393.
[36] Lisheng Xu, David Zhang, Kuanquan Wang, et al., Baseline wander correction in pulse waveforms using wavelet-based cascaded adaptive filter, Comput. Biol. Med. 37 (5) (2007) 716–731.
[37] T.R. Dawber, H.E. Thomas, P.M. McNamara, et al., Characteristics of the dicrotic notch of the arterial pulse wave in coronary heart disease, Angiology 24 (4) (1973) 244–255.
[38] K. Mustafa, A system for analysis of arterial blood pressure waveforms in humans, Comput. Biomed. Res. 30 (1997) 244–255.
[39] S.C. Millasseau, R.P. Kelly, J.M. Ritter, et al., Determination of age-related increases in large artery stiffness by digital pulse contour analysis, Clin. Sci. 103 (2002) 371–377.
[40] P. Jankowski, Integrating geographical information systems and multiple criteria decision-making methods, J. Geogr. Inf. Syst. 9 (3) (1995) 251–273.
[41] Dengfeng Li, Multiattribute decision making models and methods using intuitionistic fuzzy sets, . Syst. Sci. 70 (2005) 73–85.
[42] J.P. Brans, P.H. Vincke, A preference ranking organisation method: (the promethee method for multiple criteria decision-making), Manage. Sci. 31 (2) (1985) 647–656.